

MAX-PLANCK-INSTITUT FÜR PLASMAPHYSIK
GARCHING BEI MÜNCHEN

Stochasticity and Order in a Linear
Quasiperiodic Differential Equation

A. Salat and J. Tataronis⁺)

IPP 6/204

March 1981

⁺) University of Wisconsin, Dept. of Electrical and
Computer Engineering, Madison, Wisconsin 53 706

*Die nachstehende Arbeit wurde im Rahmen des Vertrages zwischen dem
Max-Planck-Institut für Plasmaphysik und der Europäischen Atomgemeinschaft über die
Zusammenarbeit auf dem Gebiete der Plasmaphysik durchgeführt.*

IPP 6/204

A. Salat
J. Tataronis

Stochasticity and Order
in a Linear Quasiperiodic
Differential Equation

March 1981 (in English)

Abstract

Long-time correlations in the solution of a linear second-order quasi-periodic differential equation are investigated numerically and graphically. The equation is also equivalent to an autonomous Hamiltonian system which is linear in the action variables \underline{P} and hence not amenable to KAM theory. The existence of invariant tori in six-dimensional phase space is investigated with the help of 3-d stereoscopic pictures. Both torus destruction and torus survival for finite perturbations are found.

Introduction

In the following we discuss properties of the solution of an ordinary second-order linear differential equation (1.1), whose coefficient f is a quasiperiodic function of the independent variable t .

The investigation was motivated by a study of the "continuum" in Alfvén wave propagation¹ in non-axisymmetric tori where the equilibrium is periodic in the poloidal and toroidal angles θ and ϕ , respectively. The wave propagates along the magnetic field, so that $\theta = \theta(t)$, $\phi = \phi(t)$, where t is a coordinate along the field, and $-\infty < t < \infty$ on irrational surfaces. In order to be physically acceptable, the solution must also be periodic in $\theta(t)$ and $\phi(t)$. Whether such a solution exists is unknown. Equation (1.1) represents a simplified model equation.

Independently of its origin eq. (1.1) proves to be of more general interest. It may also be written as an autonomous Hamiltonian system and one may ask whether it is integrable or not, in particular for $|f| \ll 1$. The essential point is that the results of Kolmogorov, Arnold and Moser² (KAM) cannot be used here since one of their assumptions, non-linearity in the momenta, does not hold. In particular, as an unusual feature, both the undisturbed and the disturbed Hamiltonian are linear in the momenta. We want to draw attention to this class of problems. We shall investigate it here with the "surface of section" technique³ in 6-d phase space.

1. Basic Equations and Formal Solution

We consider the differential equation

$$\ddot{\psi}(t) + [\omega_0^2 + f(t)] \psi = 0, \quad (1.1)$$

where

$$\begin{aligned}
 f(t) &\equiv f(\theta_1(t), \theta_2(t)) = \\
 &= \sum_{n=-\infty}^{+\infty} (-1)^n [F_1 \delta(t-nT_1-c_1) + F_2 \delta(t-nT_2-c_2)] \\
 &= \sum_{n=-\infty}^{+\infty} C_n \delta(t-t_n)
 \end{aligned}
 \tag{1.2}$$

is a "quasiperiodic" function of t :

$$f(\theta_1, \theta_2) = f(\theta_1 + 2\pi, \theta_2) = f(\theta_1, \theta_2 + 2\pi) \tag{1.3}$$

with

$$\begin{aligned}
 \theta_i &= \omega_i t + c_i ; \quad \omega_i = \pi/T_i ; \quad c_i = \text{const} ; \\
 & \quad i = 1, 2 .
 \end{aligned}
 \tag{1.4}$$

Equation (1.1) is an oscillator whose frequency ω_0 is modified quasiperiodically by the δ function terms. T_1/T_2 is assumed to be irrational. The shift $t \rightarrow t + 2T_i$ corresponds to $\theta_i \rightarrow \theta_i + 2\pi$. Equation (1.1) may be written in the form

$$\dot{\underline{x}}(t) = \underline{A}(\underline{\theta}(t)) \cdot \underline{x} ; \quad \underline{A}(\underline{\theta}) = \underline{A}(\underline{\theta} + 2\pi \underline{e}_i) , \tag{1.5}$$

where in the present case

$$\underline{x} = \begin{pmatrix} \psi \\ \dot{\psi} \end{pmatrix}; \quad \underline{A} = \begin{pmatrix} 0 & 1 \\ -\omega_0^2 - f & 0 \end{pmatrix}; \quad \underline{\theta} = \begin{pmatrix} \theta_1 \\ \theta_2 \end{pmatrix} \tag{1.6}$$

and \underline{e}_i are unit vectors with components 0 and 1.

Between the δ functions eq. (1.1) has the solution $\psi = a \cos \omega_0 t + b \sin \omega_0 t$. Integration across the δ functions at $t = t_n$ yields the jump conditions

$$[\psi]_{t_n} = 0 , \quad [\dot{\psi}]_{t_n} = -C_n \psi(t_n). \tag{1.7}$$

For the amplitudes a_n, b_n at $t = t_n$ one obtains the recursion

$$\begin{pmatrix} a_n \\ b_n \end{pmatrix} = \underline{T}_n \cdot \begin{pmatrix} a_{n-1} \\ b_{n-1} \end{pmatrix} = \begin{pmatrix} 1+c_n \sin 2\omega_0 t_n & 2c_n \sin^2 \omega_0 t_n \\ -2c_n \cos^2 \omega_0 t_n & 1-c_n \sin 2\omega_0 t_n \end{pmatrix} \cdot \begin{pmatrix} a_{n-1} \\ b_{n-1} \end{pmatrix}, \quad (1.8)$$

where $c_n = C_n / (2\omega_0)$. This allows fast numerical calculation of the solution, in particular of $x_n = \psi(t = t_n)$, $y_n = \dot{\psi}(t = t_n + 0)$ at the end of each jump.

2. Two-dimensional Plots

In order to determine the amount of stochasticity in the long-time behaviour of the solution we ran the system for $0 \leq n \leq N$, N being up to 10^6 , and plotted the consecutive "states" (x_n, y_n) as points on an x-y plane. To be more precise, points belonging to full periods $2T_1$ and $2T_2$ are plotted in separate figures characterized by the indices 1 and 2, respectively. Half-period points were omitted. The origin is at the centre. The values 0 and ± 1 are indicated at the margin. Each plot corresponds to a single sequence of points, usually starting at $x_0 = 1, y_0 = 0$. A selection of typical cases is shown in Figs. 1 to 7. The parameters T_i, F_i are normalized by setting $\omega_0 = 1$.

The amount of stochasticity considerably varies from one case to the other. Figure 1 corresponds to a high degree of stochasticity. It was obtained by a random choice of parameters. Other cases such as Fig. 5.1 show considerable correlations. Figures 6 and 7 present a set of one-dimensional curves or even discrete points. Generally speaking, it takes much more time to find strongly non-stochastic cases, by trial and error, than stochastic ones, and they may be sensitive to variations in T_i of less than 0.01 %!

Figures 6.1 and 7.1, although similar in appearance, are very different. When the number N of recursions is increased, more and more segments are created in cases 6.1 and 6.2, while Fig. 7 remains unchanged even for extremely large N . Figures 3 and 4 correspond to weakly unstable cases. In case 3 the sequence initially converges towards the origin before its final slow exponential divergence. There also exist strongly unstable cases with just a few points on the plot. In most stable cases the region occupied reaches its final size after a few thousand iterations.

If a solution of eq. (1.1) exists which has the same quasiperiodicity as the perturbation f , it is easily recognized on the plots. From $\psi(t) = u(\theta_1(t), \theta_2(t))$, where u is a quasiperiodic function which obeys eq. (1.3), it follows that in the figures either θ_1 or θ_2 is const, mod 2π , and both ψ and $\dot{\psi}$ are periodic in the complementary variable. Therefore, for $N \rightarrow \infty$, the sequence of points forms a closed curve. No such solution has been found so far. Case 7, however, is a subharmonic solution with periods 2π and $\pi/4$ in θ_1 and θ_2 , respectively, as closer inspection reveals. Case 6 is difficult to interpret because of its unsteady nature with increasing N .

3. Parameter Studies and General Properties

Equation (1.1) contains four parameters T_1, T_2, F_1, F_2 so that an exhaustive parameter study is difficult. Some general conclusions, however, may be given.

It is useful to consider the special case of a periodic perturbation by, say, setting $F_2 = 0$. In this case the Floquet-Ljapunov theory⁴ states that $\psi(t)$ is of the form

$$\psi = e^{\pm i\nu t} u(\theta_1(t)), \quad (3.1)$$

with $u(\theta_1) = u(\theta_1 + 2\pi)$, ν^2 real, and ν follows from the

knowledge of a fundamental solution of eq. (1.1) after one full period, $t = 2T_1$. (From eq. (3.1) it follows that the resulting figures (.1) of the last section would be closed curves, while figs.(.2) in general would not.) With eq. (1.8) v may be obtained analytically. The resulting stability diagram, $v^2 < 0$ corresponding to instability, is shown in Fig. 9. The pattern repeats periodically in $\Delta\omega_0 T_1 = \pi$. Instability sets in at the points $(2n+1)\omega_1 = 2\omega_0$, $n = 0, \pm 1, \dots$

It turns out that for quasiperiodic perturbations as well the solution is (strongly) unstable if F_1 or F_2 is large enough, or if either T_1 or T_2 is inside an unstable region and F_1, F_2 are comparable in size. For $F_1/\omega_0 = F_2/\omega_0 = 0.5$ we looked for strongly unstable behaviour on a coarse T_1, T_2 grid. About one-third of all cases were found to be unstable. The majority, but not all unstable cases, closely corresponded to the relation

$$m\omega_1 + n\omega_2 = r\omega_0, \quad (3.2)$$

m, n, r being integers, with absolute values ≤ 3 . The most conspicuous correlation is with $\omega_1 + \omega_2 = 2\omega_0$ (apart from the above-mentioned $(2n+1)\omega_i = 2\omega_0$). The amplitudes F_i , however, also play a nontrivial role. For $\omega_0 T_1 = 0.998$, $\omega_0 T_2 = 0.7574$, for example, hence $\omega_2 - \omega_1 \approx \omega_0$, there is a sickle-shaped (weakly) unstable region around $\sqrt{F_1^2 + F_2^2} \approx 0.6 \omega_0$, with stability for both larger and smaller amplitudes; (compare cases 2 and 3).

We investigated how the distance δ_n of two neighbouring starting points changes in time by calculating the Kolmogorov-Sinai (KS) entropy ⁵:

$$S = \frac{1}{N} \sum_{n=1}^N \ln \frac{\delta_n}{\delta_{n-1}} \quad (3.3)$$

for large N . For stable cases, with all initial values tested, its absolute value converges to zero. This has

to be expected since linearity of eq. (1.1) together with stability of the solution exclude the existence of a diverging sequence of δ_n . "Local" mixing instability⁵ thus does not occur.

4. Hamiltonian and Related Viewpoints

In order to obtain a better understanding of the properties of eq. (1.1), more general viewpoints are helpful.

A general investigation whether linear (and non-linear) systems of quasiperiodic differential equations of the form (1.5) are reducible has been made by Bogoljubov, Mitropolskii and Samoilenko (BMS)⁶. Equation (1.5) is "reducible" if an ansatz $\underline{x}(t) = \underline{U}(\underline{\theta}(t)) \cdot \underline{y}(t)$, $\underline{U}(\underline{\theta}) = \underline{U}(\underline{\theta} + 2\pi \underline{e}_1)$ with quasiperiodic matrix function \underline{U} yields $\underline{y} = \underline{K} \cdot \underline{y}$, where \underline{K} is a constant matrix. Reducibility is thus a generalization of Floquet-Ljapunov properties to the quasiperiodic case, and determines the type of solution. The BMS theory considers small quasiperiodic perturbations, $\underline{A} = \underline{A}_0 + \underline{A}_1(\underline{\theta})$, $\underline{A}_0 = \text{const}$, $\underline{A}_1 = O(\varepsilon \ll 1)$, and employs the method of accelerated convergence of the perturbation series as developed by Kolmogorov, Arnold and Moser (KAM)². Very briefly speaking, BMS show that the measure of reducible matrices \underline{A} is finite and tends to 1 for $\varepsilon \rightarrow 0$, and that for any \underline{A}_0 there is a slightly different reducible \underline{A}_0 , provided the frequencies involved - $\omega_0, \omega_1, \omega_2$ in our case - are sufficiently incommensurate and the perturbation is smooth enough. In addition, BMS have proved reducibility under similar conditions, provided the eigenvalues of \underline{A}_0 have a real part, which, however, does not hold in our case (ω_0 real). Consequently, BMS theory gives us no explicit results.

There is a more direct connection of eq. (1.1) with KAM theory. By introducing the canonical variables $q_0 = \psi, p_0 = \dot{\psi}$, which are transformed to Q_0, P_0 by

$q_0 = \sqrt{2P_0/\omega_0} \cos Q_0$, $p_0 = -\omega_0 \sqrt{2P_0/\omega_0} \sin Q_0$, and the canonical coordinates

$$Q_i = \omega_i t + c_i, \quad i = 1, 2 \quad (4.1)$$

equation (1.1) may be written as an autonomous Hamiltonian system with canonical variables $\underline{P} = (P_0, P_1, P_2)$ and $\underline{Q} = (Q_0, Q_1, Q_2)$ as follows

$$H(\underline{Q}, \underline{P}) = \sum_{\alpha=0}^2 \omega_\alpha P_\alpha + \frac{P_0}{\omega_0} \cos^2 Q_0 \cdot f(Q_1, Q_2) \quad (4.2)$$

with $f(Q_1, Q_2) = f(Q_1 + 2\pi, Q_2) = f(Q_1, Q_2 + 2\pi)$. The advantage of introducing two coordinates to make H time-independent is that as a result $P_\alpha, Q_\alpha, \alpha = 0, 1, 2$, are conjugate action and angle variables for the undisturbed Hamiltonian $H_0 = H(f=0)$. $Q_\alpha, \text{ mod } 2\pi$, are angles on 3-dimensional "torus surfaces" $P_\alpha = \text{const}, \alpha = 0, 1, 2$, which are embedded in the 6-dimensional phase space. KAM theory discusses the survival of invariant tori in phase space, i.e. integrability, when a small perturbation, $|f| \ll 1$ here, is applied. Unfortunately, KAM theory requires that $\det (\partial^2 H_0 / \partial P_i \partial P_j) \neq 0$ (or an equivalent condition). This condition, however, does not hold here since H_0 is linear in \underline{P} . Moreover, the perturbation $\Delta H = H - H_0$ is also linear. Therefore, techniques to obtain a nonlinear \tilde{H}_0 to some higher order in f from the nonlinearity in ΔH do not work here. Integrability of such "completely degenerate" Hamiltonians has not, to our knowledge, been investigated before. (Note that H is integrable if f is periodic in t , according to the Floquet theory; integrability is uncertain only for quasiperiodic f .)

In order to decide whether invariant tori exist, we use the following surface of section technique appropriate to our 6-dimensional problem: Let us assume H to be completely integrable. Then, by definition, apart from $H(\underline{Q}, \underline{P}) = \text{const}$, two additional invariants of motion exist,

$I_i(Q, P) = \text{const}$, $i = 1, 2$. They may be used in principle to express two variables, e.g. P_2, Q_2 , in terms of the other ones. One invariant, indeed, always exists:

$I_1(Q_1, Q_2) = Q_1/\omega_1 - Q_2/\omega_2$, from the definition (4.1). In addition, we make a cut at $Q_1 = 0, \text{mod } 2\pi$. (Compare with a cut at a fixed toroidal angle of a 2-d torus in 3-d space.) If invariant tori exist, the trajectories crossing the cut still form a smooth manifold on it³. From $H = \text{const}$ the manifold follows in the form (with Q_0, P_0 transformed into q_0, p_0)

$$h(q_0, p_0, P_1) = \text{const}, \quad (4.3)$$

where $q_0 = \psi$, $p_0 = \dot{\psi}$ and P_1 are taken at $t = n \cdot 2T_1$. Equation (4.3) represents a 2-d surface in q_0, p_0, P_1 space, in the limit $t \rightarrow \infty$. (A cut at $Q_2 = 0, \text{mod } 2\pi$ is analogous.) Thus, if the points $(x_n = \psi, q_n = \dot{\psi}, z_n = P_1)$ at $t = n \cdot 2T_1$ lie on a smooth surface, H is integrable, and a torus is preserved. Conversely, if the sequence of points fills a volume, H is not integrable. The method of visualizing $(\psi, \dot{\psi}, P_1)$, and the results are presented in the next section.

Equation (4.3) requires a knowledge of P_1 or P_2 . They follow from the canonical equations

$$\dot{P}_i = - \frac{\partial H}{\partial Q_i} = - \frac{q_0^2}{2} \frac{\partial}{\partial Q_i} f(Q_1, Q_2), \quad i = 1, 2 \quad (4.4)$$

By integration over the δ functions and partial integration one obtains for the jump of P_i

$$\begin{aligned} [P_i] &= \int dt \dot{P}_i = - \frac{1}{2} \int dt q_0^2 \frac{\partial}{\partial \omega_i t} f(\omega_1 t, \omega_2 t) = \\ &= \frac{1}{\omega_i} \int dt q_0 \dot{q}_0 f = - \frac{1}{\omega_i} \int dt p_0 \dot{p}_0 = - \frac{1}{2\omega_i} [p_0^2] \end{aligned} \quad (4.5)$$

where $\dot{q}_0 = p_0$, $\dot{p}_0 = -(\omega_0^2 + f)q_0$ have been used and jumps at $t_n = 2nT_i$ only contribute. $[p_0^2]$ follows from eqs. (1.7), (1.8).

5. Three-dimensional Plots

In order to find out whether a numerically computed sequence of points with the Cartesian coordinates (x_n, y_n, z_n) fills a volume or lies on a smooth surface the usual methods of level lines or perspective drawing are hardly applicable here because the (x_n, y_n) values are not located on a fixed grid. Therefore, we chose to represent the sequence of points direct by a stereoscopic technique. Two conjugate plots are made from the sequence, each being a projection under a slightly different viewing angle. For better inspection the whole sequence is also tilted and turned 45° counter clock wise. The double plot should be viewed not by fixing the eyes on the points but by "looking through" them and fixing at infinity. With some training a very pronounced stereoscopic impression is created. Sometimes it is helpful to put a white sheet between the eyes and the centre of the double plot.

In Figs. 1.3 - 8.3 we present a selection of cases with typical behaviour. For most cases the corresponding two-dimensional figures were discussed in Section 2, Figs. 1.1 - 7.1. The ellipse is a projection of the reference unit circle. The sequence of points starts with the initial value $(1, 0, b)$, where b is an arbitrary convenient "base". The number of iterations is called N_3 . In order to make the position of points more obvious, the z coordinate is either slightly compressed, or magnified by a factor s ranging from 0.67 to 20.

The cases (8.3) and (1.3) correspond to randomly chosen parameters. The figures show a ribbon-like structure and a thin, curved disk with a hole, respectively. A cushion-like structure with holes and a fence-like structure are visible in Figs. 2.3 and 5.3. The curve segments of case 6.3 seem to lie on a "bee-hive". In most cases the points do not yield a surface but fill a finite volume. H in these cases is non-integrable. The deviation from a surface, however, is relatively small in many cases,

not only for nearly periodic ones. In Fig. 7.3, however, well defined surfaces (looking like curtains) are obtained so that integrability is proved.

Similarly to the horizontal dimensions, the final size of the vertical extension in stable cases is reached at about $N_3 = 5 - 10,000$ iterations.

Integrability should be investigated for different initial values (\bar{Q}, \bar{P}) in phase space. The effects of \bar{P}_1 , \bar{P}_2 and of one of the \bar{Q}_1 , \bar{Q}_2 are trivial. The absolute value of the vector (\bar{q}_0, \bar{p}_0) is also irrelevant since, owing to the linearity of eq. (1.1) and owing to eq. (4.4), $(\alpha\psi, \alpha\dot{\psi}, \alpha^2 P_1)$ is a solution if $(\psi, \dot{\psi}, P_1)$ is. It remains to check the effects of the direction of the vector (\bar{q}_0, \bar{p}_0) and of the phase difference between Q_1 and Q_2 , corresponding to $c_1 - c_2$ in eq. (1.2). In all cases investigated we found that only minor details of the solution are affected, while the type of the solution remains unchanged ($c_1 = c_2 = 0$ in Figs. 1-8).

In conclusion, concerning integrability of Hamiltonian H , eq. (4.2), our results are: Depending on the parameters T_1 , T_2 and F_1 , F_2 , H is either integrable in the whole phase space, or is nonintegrable everywhere in phase space. Nonintegrability seems to occur more often.

Acknowledgements:

The authors would like to thank H. Tasso and D. Pfirsch for helpful discussions.

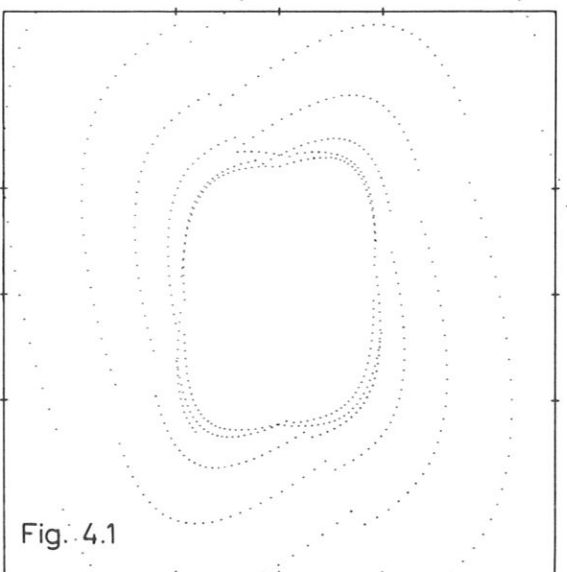
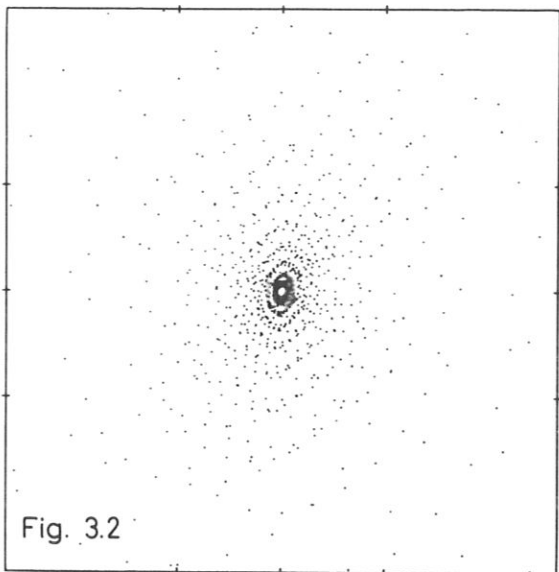
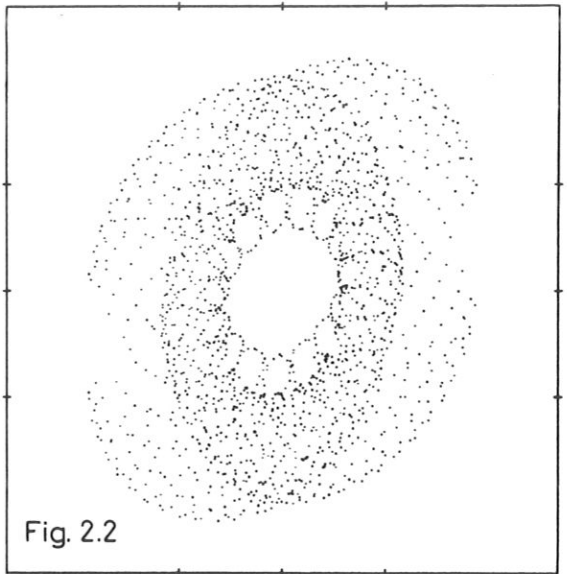
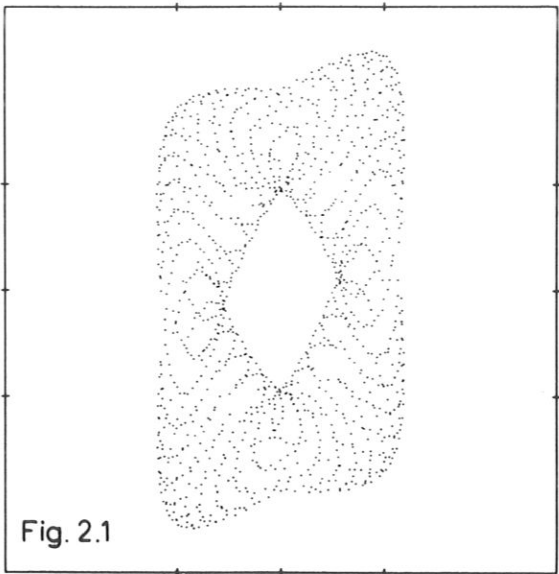
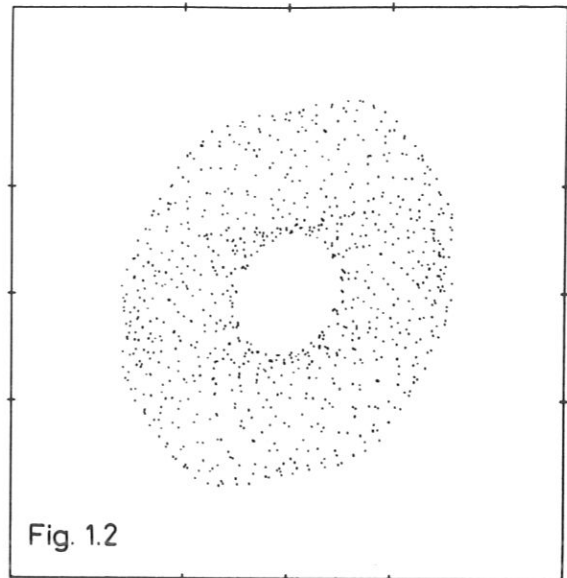
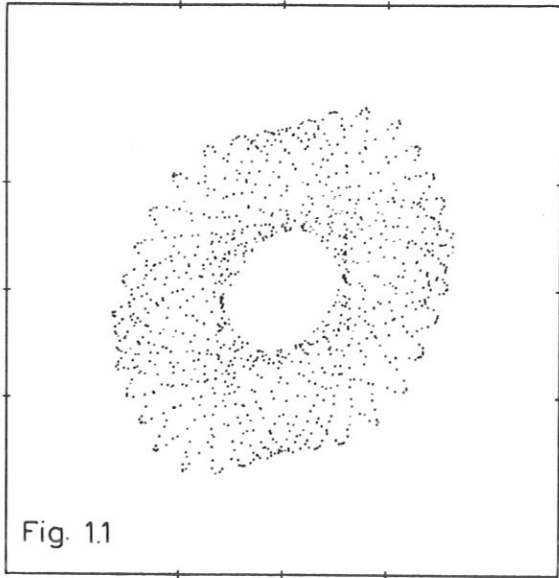
This work was performed under the terms of the agreement on association between the Max-Planck-Institut für Plasmaphysik and EURATOM.

References

- 1 Tataronis, J.A., Talmadge, J.N. and Shohet, J.L., "Alfvén Wave Heating in General Toroidal Geometry", Univ. of Wisconsin Report ECE-78-10 (1978)
- 2 As a review, see: M.V. Berry in Topics in Nonlinear Dynamics, Ed. Siebe Jorna, American Institute of Physics, New York, (1978);
Whiteman, K.J., Rep. Progr. Phys. 40, 1033-1069 (1977)
- 3 Arnol'd, V.I. and Avez, A., Ergodic Problems of Classical Mechanics, Benjamin W., New York (1968)
- 4 Yakubovich, V.A. and Starzhinskii, V.M., Linear Differential Equations with Periodic Coefficients, John Wiley and Sons, Inc., New York, (1975)
- 5 Chirikov, B.V., Phys. Reports 52, 263-379 (1979)
- 6 Bogoljubov, N.N., Mitropolskii, Ju., A. and Samoilenko, A.M., Methods of Accelerated Convergence in Nonlinear Mechanics, Springer Verlag, Berlin, (1976)
- 7 Ford, J. and Lemsford, G.H., Phys. Rev. A 188 (1970) 416;
Lichtenberg, A.J., in "Stochastic Behavior in Classical and Quantum Hamiltonian Systems", Eds. Casati G. and Ford J., Springer Verlag, Berlin (1979).

Figure Captions

- Fig. 1 Solution $(\psi, \dot{\psi})$ at $t = 2nT_1$ (Fig. 1.1) and $t = 2nT_2$ (Fig. 1.2). Stereoscopic view of $(\psi, \dot{\psi}, P_1)$ (Fig. 1.3). For $T_1 = \sqrt{8.5}$, $T_2 = \sqrt{13}$, $F_1 = 0.5$, $F_2 = 0.4$; $N = 4000$, $N_3 = 5000$, $s = 0.67$.
- Fig. 2 $T_1 = 0.998$, $T_2 = 0.7574$, $F_1 = 0.5$, $F_2 = 0.4867$; $N = 6000$, $N_3 = 6000$, $s = 0.67$.
- Fig. 3 $T_1 = 0.998$, $T_2 = 0.7574$, $F_1 = 0.5$, $F_2 = 0.4512$; $N = 4000$. Weakly unstable.
- Fig. 4 $T_1 = 1.027$, $T_2 = 0.77398$, $F_1 = 0.3$, $F_2 = 0.281$; $N = 6000$. Weakly unstable.
- Fig. 5 $T_1 = 0.74844$, $T_2 = 2.919144$, $F_1 = 0.7$, $F_2 = 0.7$; $N = 8000$, $N_3 = 5000$, $s = 0.67$.
- Fig. 6 $T_1 = 1.045$, $T_2 = 0.7842$, $F_1 = 0.1$, $F_2 = 0.1$; $N = 8000$, $N_3 = 10\ 000$, $s = 6.67$.
- Fig. 7 $T_1 = 1.027$; $T_2 = 0.773969$, $F_1 = 0.1$, $F_2 = 0.284$; $N = 8000$, $N_3 = 6000$, $s = 20$
- Fig. 8 $T_1 = 0.5$, $T_2 = \sqrt{0.3}$, $F_1 = 0.5$, $F_2 = 0.1$; $N_3 = 4000$, $s = 16.67$.
- Fig. 9 Stability diagram for periodic perturbation



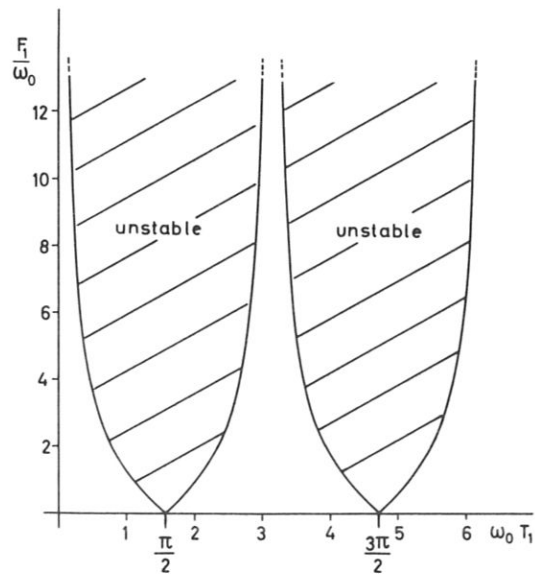
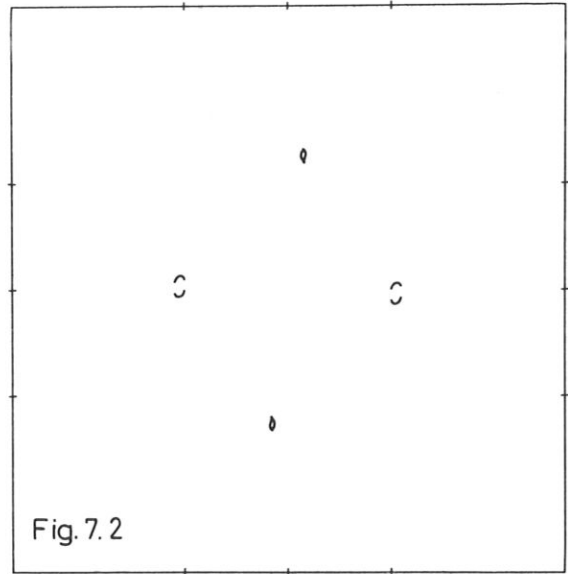
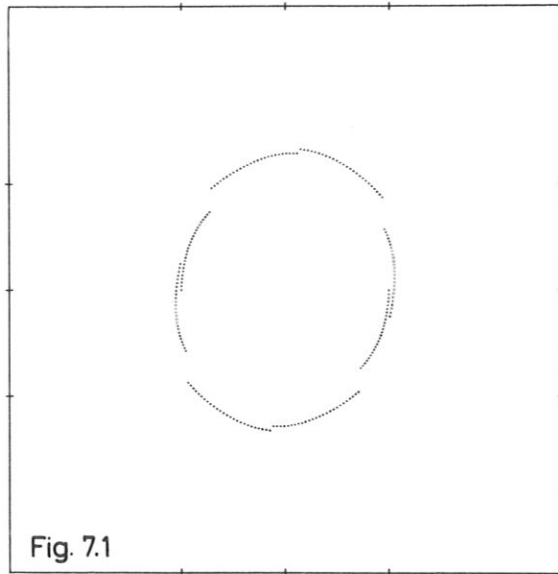
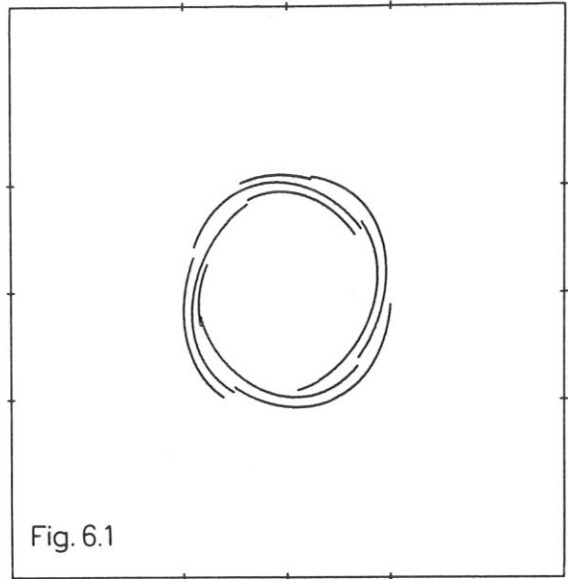
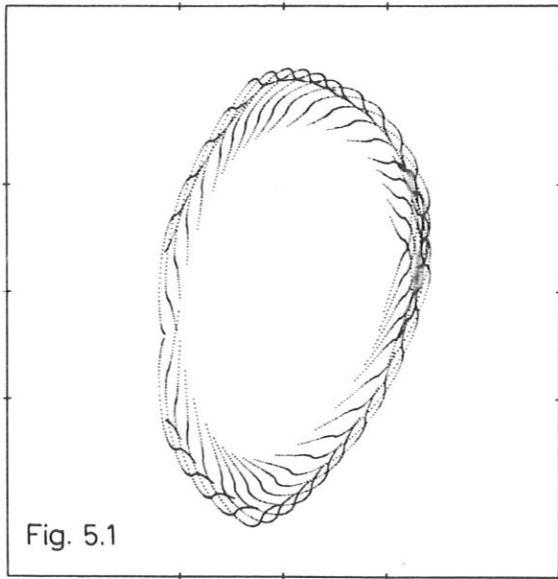


Figure 9

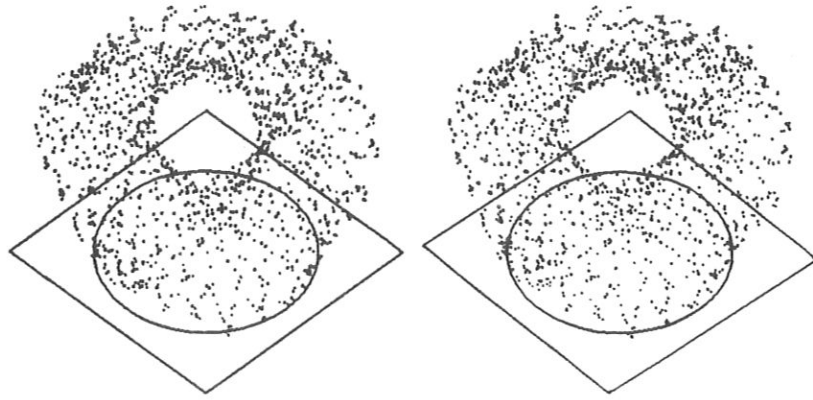


Fig. 1.3

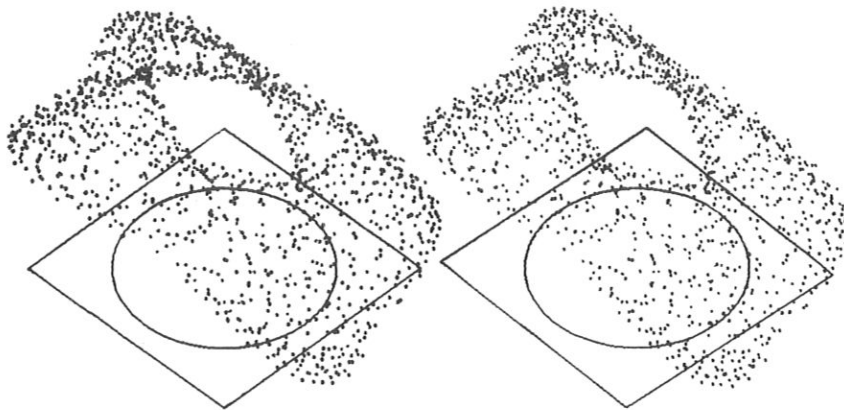


Fig. 2.3

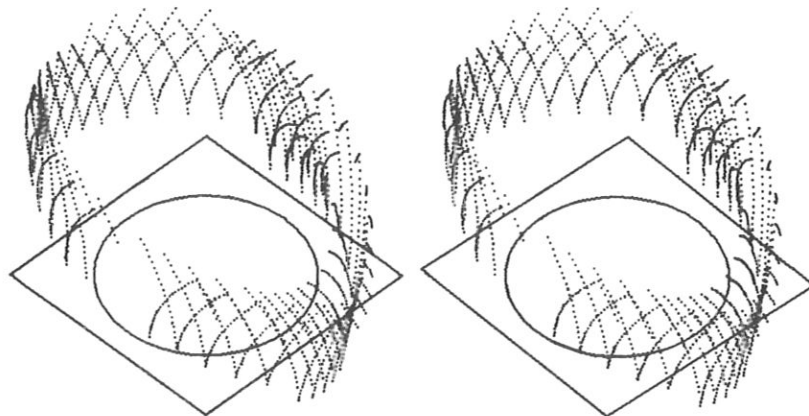


Fig. 5.3

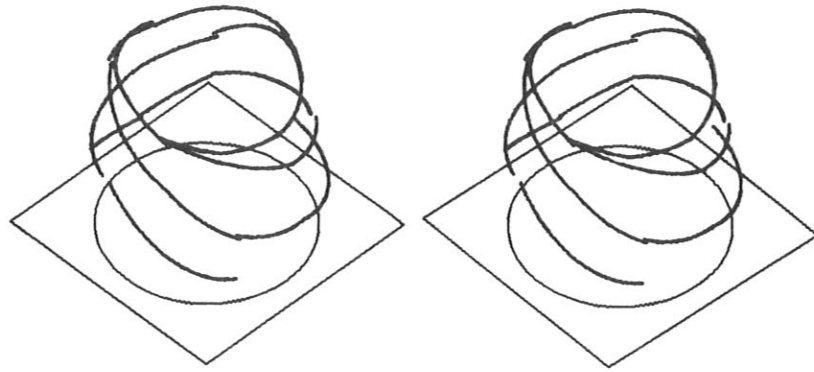


Fig. 6.3

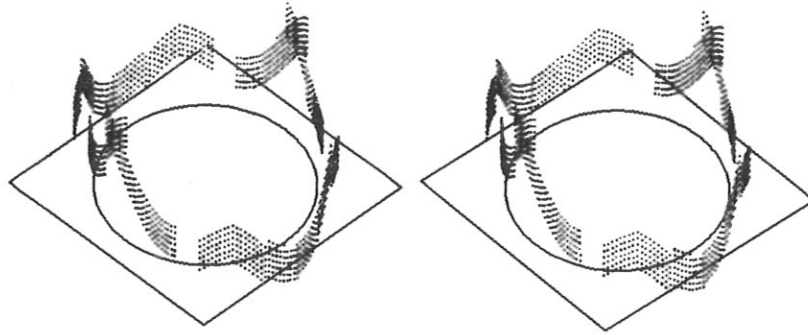


Fig. 7.3

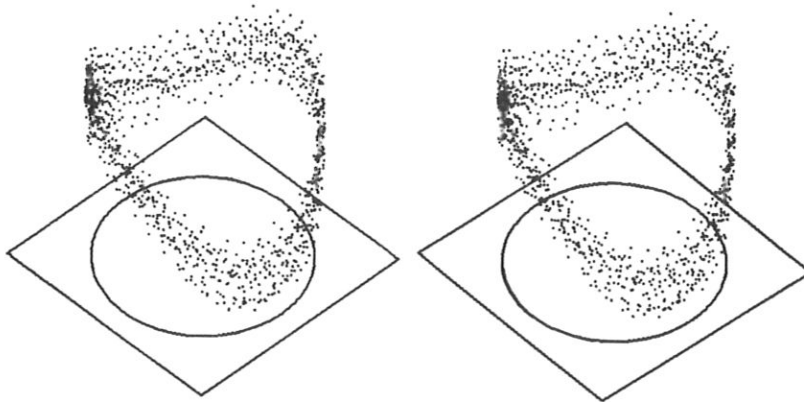


Fig. 8.3